Upper bound of tunnel face stability using asymmetric yielding

Elkayam, Itai; Klar, Assaf

Published in:
Underground Space

Link to article, DOI:
10.1016/j.undsp.2018.03.001

Publication date:
2018

Document Version
Version created as part of publication process; publisher's layout; not normally made publicly available

Available online at www.sciencedirect.com

ScienceDirect

Underground Space xxx (2018) xxx–xxx

www.elsevier.com/locate/undsp

Upper bound of tunnel face stability using asymmetric yielding

Itai Elkayam [a,1], Assaf Klar [b,*,2,3]

[a] Technion – Israel Institute of Technology, Haifa, Israel
[b] Technical University of Denmark, Lyngby, Denmark

Received 29 October 2017; received in revised form 16 February 2018; accepted 8 March 2018

Abstract

Although significant advancement has been made over recent years with respect to three-dimensional upper bound calculations of tunnel facing, a considerable difference still exists between analytically and empirically based stability values. The current work suggests that the difference may well be the outcome of the traditional use of Tresca yield criterion for the upper bound calculations, which, by definition, does not distinguish between the shearing modes (compression, extension, plane strain). Consequently, this paper suggests and discusses a new yield function, which allows for asymmetric yielding. Such yielding is only beneficial in case of three-dimensional and continuous velocity fields, and therefore a numerical procedure that generates relevant kinematically admissible fields for classical upper bound calculation is suggested. The procedure involves conversion of a load controlled boundary value problem to a velocity controlled problem at the limit state of collapse. The analysis results in significantly lower upper bound values than those presented earlier (for Tresca material), and much closer to the stability curves of Kimura and Mair (1981), commonly used in design.

Keywords: Tunnels; Plasticity; Stability; Upper bound

1. Introduction

The use of underground space has increased significantly over the last few decades together with an improvement in tunneling techniques and quality. Nonetheless, unfortunate events of tunnel collapse still occur. The most critical time for soil instability and potential collapse occurs before lining placement, when an unlined heading area is either completely unsupported or partly supported by constant air or fluid pressures. Considering collapse may well be the most dangerous scenario of tunnel construction, it is no wonder that significant research effort has been placed over the years to evaluate both analytically and experimentally the limit state of tunnel stability.

This paper deals with the problem of tunnel face stability in undrained clay, and does not address stability problems of frictional and dilative materials (e.g., Atkinson and Potts, 1977; Leca and Dormieux, 1990; Pan and Dias, 2016; Zhang et al., 2015).

For cohesive soils, the limit state is characterized by a stability number, N, describing the critical ratio between pressures and weight to soil strength:

$$N = \frac{\sigma_S - \sigma_T + \gamma(C + D/2)}{s_u} \tag{1}$$

where σ_T and σ_S are the normal stresses acting on the tunnel face and on the ground surface, respectively, γ is the unit weight of the soil, C is the tunnel cover depth, D is the diameter of the tunnel, and s_u is the undrained shear strength of the soil. The above definition is classically

* Corresponding author.
E-mail address: askla@byg.dtu.dk (A. Klar).
[1] Research Associate, National Building Research Institute, Technion – Israel Institute of Technology.
[2] Professor, Department of Civil Engineering, Technical University of Denmark (DTU).
[3] On sabbatical leave from the Technion – Israel Institute of Technology.

https://doi.org/10.1016/j.undsp.2018.03.001

attributed to homogeneous soils, whereas for inhomogeneous soils the strength at a representative depth is selected. Most of the upper bound solutions developed over the years focused on plane strain conditions (e.g. Augarde et al., 2003; Osman et al., 2006; Sloan and Assadi, 1993; Wilson et al., 2013; Xiang and Song, 2017), most likely due to the three dimensional complexity involved with tunnel face stability. Yet, a few solutions for the more complicated 3D problem exist.

Davis et al. (1980) were among the first to establish stability numbers for a circular tunnel heading, using both the lower and the upper bound theorems. Their stability numbers based on the upper bound theorem range between 8.4 and 18.7 for C/D between 1 and 4. Klar et al. (2007) have formulated a 3D continuous mechanism based on an incompressible 'elastic' flow field and derived similar upper bound values. The mechanism velocity field is essentially the same as that solved using incompressible viscous flow, because there is an analogy between the field equations of the two cases. Mollon et al. (2010) developed a multiple rigid-block mechanism to establish upper bound values, which also vary in a similar trend. An impressive attempt to reduce the upper bound solution has been made by Mollon et al. (2013), who formulated two ingenious continuous mechanisms which were solved by a mixed analytical-numerical approach, involving velocities along curvilinear coordinates. They, however, used in their upper bound calculations an approximated strain tensor that is based on an orthogonal homogeneous coordinate system together with the velocities from the curvilinear coordinate system, thus ignoring straining along orthoradial lines due to radial displacements. Using this approach they were able to reduce the upper bound values. However, their stability numbers may not be considered strict upper bound solutions due to the approximated nature of the strain tensor. The exact representation of the curvilinear strain rate tensor together with a closed form solution for Mollon et al. (2013)'s mechanisms were provided by Klar and Klein (2014). The adjusted upper bound values of Mollon et al. (2013)'s mechanisms, considering the complete strain tensor, fall in a similar range to those of previous solutions, without the significant decrease hoped for. Recently, Zhang et al. (2017) followed the work of Klar and Klein (2014) and provided, with the same general mechanism, stability numbers also for cases in which the strength increases linearly with depth.

In all of the above analytical works, the Tresca yield criterion was used to represent soil yielding (i.e. $f = |\sigma_1 - \sigma_2| + |\sigma_2 - \sigma_3| + |\sigma_3 - \sigma_1| - 4s_u = 0$, where σ_1, σ_2 and σ_3 are principal stresses and s_u is the undrained shear strength), leading to a dissipation rate of $2s_u|\dot{\epsilon}|_{max}$ per unit volume and $s_u|\delta v|$ per unit area along velocity discontinuities (where $|\dot{\epsilon}|_{max}$ is the absolutely largest principal component of the plastic strain rate and δv is the velocity jump).

Although an advancement has been made with respect to the analytical evaluation of the stability numbers, routine design still utilizes the empirically based stability curves of Kimura and Mair (1981), most probably because they lie significantly below the upper bound values. Fig. 1 shows the empirical stability values and those of the aforementioned analytical solutions. As can be seen, all of the analytical values are found within a rather narrow band significantly above the empirical values. It may be claimed that this is due to the fact that the values are based on the upper bound theorem and further work is required to find more representative mechanisms (and lower stability numbers). However, a different logical explanation may be attributed to this gap.

The main goal of Klar and Klein (2014) was not to establish new stability numbers, but rather to utilize the continuous mechanisms to evaluate the surface deformation and volume loss under working conditions based on energy principles as part of the mobilized strength design method (e.g. Klar and Osman, 2008; Klar and Randolph, 2008; Osman et al., 2006). In their work Klar and Klein (2014) recognized that all elements within the tunnel face collapse mechanism experience extension mode of deformation. That is, two of the eigenvalues of the strain rate tensor (i.e. principal strains) are in compression while the third is in extension (which due to incompressibility has the largest absolute value among the principal strains). However, the Tresca yield criterion does not distinguish between compression and extension and provides the same undrained shear strength for both modes. In reality soil exhibits smaller undrained shear strength in extension. For example, test results of Gasparre (2005) and Nishimura (2005) for London Clay showed that the ratio between extension strength and compression strength ranges between 0.67 and 0.75 with depth (average value of 0.72). The difference between extension and compression undrained strength values in clays is not new nor limited to London Clay. For example, a ratio of 0.75 between the two was recognize by Duncan and Seed (1966) for San Francisco Bay Mud, and a ratio of 0.71 by Campanella and Vaid (1973) for Haney Clay.

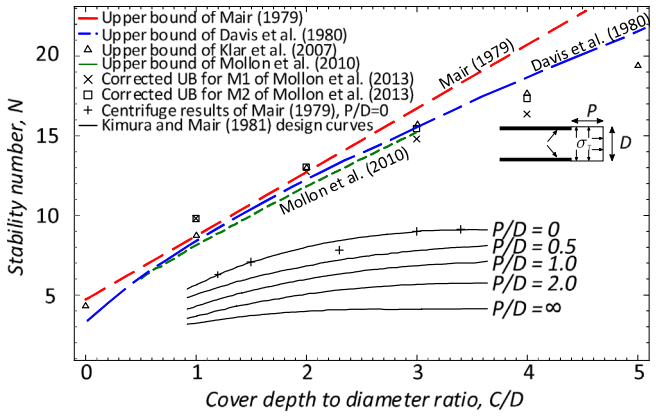

Fig. 1. Tunnel stability values based on various upper bound analyses and design curves based on centrifuge test results.

Please cite this article in press as: Elkayam, I., & Klar, A., Upper bound of tunnel face stability using asymmetric yielding, Underground Space (2018), https://doi.org/10.1016/j.undsp.2018.03.001

The difference between undrained shear strength values in extension and compression may explain the gap between the upper bound solutions and the centrifuge test results, because upper bound calculations using Tresca yield criterion cannot capture the difference in undrained shear strength.

It should be noted that Kimura and Mair (1981)'s design curves are based on Mair (1979)'s centrifuge experimental results, which were normalized by the estimated extension strength, and that the above claim should not hold under this circumstance. However, later works (which also validate Kimura and Mair (1981)'s design curves using field data) refer to the compression strength or do not explicitly mention the extension strength. The same is true to the work of Kimura and Mair (1981), which does not state the nature of the shear strength. This ambiguity, for itself, suggests that specific analytical and experimental studies, focusing on this feature, are in order.

One should recall that an upper bound analysis with a Tresca yield criterion using an 'extension undrained shear strength' (for s_u) cannot generally be considered a strict upper bound solution because it may underestimate strength (and dissipation) for elements which are not in pure symmetric extension. Therefore, one cannot simply adopt the undrained extension strength for calculation. Nonetheless, upper bound solutions can still be established by considering an asymmetric yield criterion which takes into account the variation of strength as a function of the shearing mode.

This topic was recently discussed in EURO:TUN2017 (Klar and Elkayam, 2017), and this paper further extends the work with more details regarding the analysis and more analysis cases aiming at reducing the aforementioned gap.

2. TEKJ2J3 yield criterion

A rigorous upper bound calculation requires a kinematical admissible field which involves plastic flow that is associative with the yield criterion (Davis and Selvadurai, 2005); that is an associated flow rule. This means that for upper bound calculations involving undrained shearing, the yield function for a given soil element should be independent of the confining stress, resulting in zero volumetric strain in plastic flow, due to the normality condition. Note that the size of the yield surface may still be depth dependent, thus allowing for the soil strength to be a function of the initial confining stress. This aspect, of depth dependency is not considered in the current work which is limited to a homogeneous strength field. The Tresca and von Mises yield criteria are commonly used for upper bound analyses of undrained materials, but they do not exhibit any difference of strength (or dissipation rate) between compression and extension shearing modes. In general, the effect of shearing mode on strength is apparent both in isotopic (remolded) clays and in (stress induced or inherent) anisotropic clays, although to a different extent. In anisotropic material the orientation of the principal direction to the clay platelets may be of relevance. This paper, however, focuses on the condition in which shearing mode plays the most crucial role, without considering the orientation of the bedding.

To consider the effect of different shearing modes, an asymmetric yield function, named TEKJ2J3, is suggested. It is suitable for upper bound calculations of undrained soil (zero volumetric strain).

$$f(J_2,J_3,s_u,k)=\sqrt{3J_2}-2s_u\left(1-\frac{3}{2}(1-k)\frac{2J_2^{3/2}-3\sqrt{3}J_3}{4J_2^{3/2}-3\sqrt{3}J_3}\right)=0 \tag{2}$$

where J_2 and J_3 are the basic invariants of the stress deviator ($J_2=s_{ij}s_{ij}/2$ and $J_3=s_{ij}s_{jk}s_{ki}/3$), s_u is the undrained shear stress under triaxial compression, and k is the ratio between the extension and compression undrained triaxial strength values. When $k=1$ the model degenerates into the von Mises yield criterion. Fig. 2 shows its projection on the π-plane together with the Tresca yield criterion. Since the function is independent of the confining stress, this image is correct for any confining stress, as does the Tresca yield criterion (that is, the size of the projection is the same for any given π-plane). Fig. 3 illustrates the yield criterion in the principal stress space. As can be seen, no dependency on the confining stress exists, inferring the function can be used for undrained analysis. That is, normal vectors to the yield surface illustrated in Fig. 3, which represent strain rate directions, will not produce any volumetric deformation. The yield surface remains convex as long as k is larger than 0.68, inferring that for practical use for upper bound calculations k should be in the range of $0.68 \leqslant k \leqslant 1$, since the upper bound theorem requires convexity of the yield function. As stated earlier most clays are associated with k of approximately 0.7, and this values is chosen for further analysis.

Let us examine the strength and energy dissipation, under different shearing modes, which result from this yield function together with an associative plastic flow. For triaxial compression state (i.e. $\dot{\epsilon}_{\mathrm{I}}=|\dot{\epsilon}|_{max}$ and $\dot{\epsilon}_{\mathrm{II}}=\dot{\epsilon}_{\mathrm{III}}=-0.5|\dot{\epsilon}|_{max}$), the shear strength (i.e. $(\sigma_{\mathrm{I}}-\sigma_{\mathrm{III}})_f/2$) is s_u and

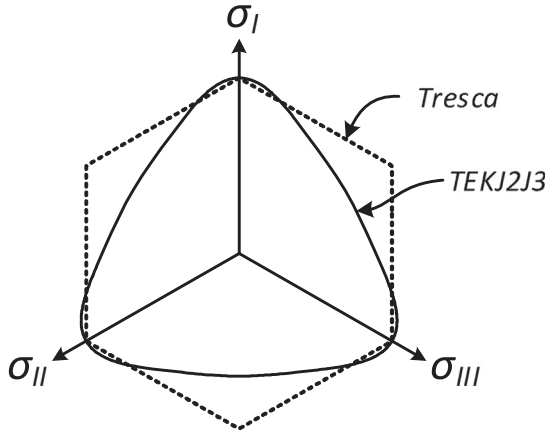

Fig. 2. TEKJ2J3 yield function for $k=0.7$: projection on the π-plane together with the Tresca yield criterion.

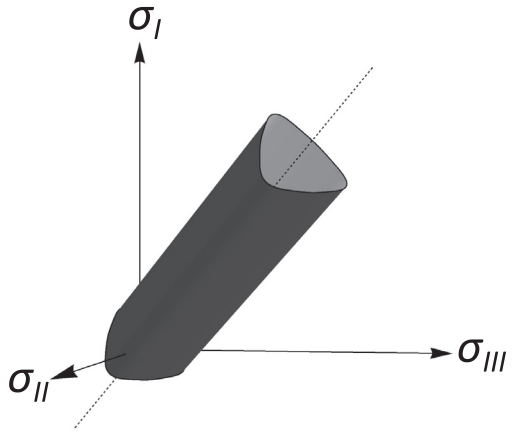

Fig. 3. TEKJ2J3 yield surface in the principal stress space ($k = 0.7$).

the rate of plastic work is $2s_u|\dot{\epsilon}|_{max}$, just as in Tresca material. Note that the roman numerals I, II, and III are used to denote major, intermediate and minor principal stresses (or strains), whereas the Hindu-Arabic numerals to indicate 3 principal stresses (or strains) without specific information about their relative magnitude. For triaxial extension state, i.e. $\dot{\epsilon}_{\mathrm{I}} = \dot{\epsilon}_{\mathrm{II}} = 0.5|\dot{\epsilon}|_{max}$ and $\dot{\epsilon}_{\mathrm{III}} = -|\dot{\epsilon}|_{max}$ the shear strength $(\sigma_{\mathrm{I}} - \sigma_{\mathrm{III}})_f/2 = ks_u$ and the rate of plastic work is $2ks_u|\dot{\epsilon}|_{max}$; that is, k times smaller than that of Tresca material. For plane strain condition (i.e. $\dot{\epsilon}_{\mathrm{II}} = 0$ and $\dot{\epsilon}_{\mathrm{I}} = -\dot{\epsilon}_{\mathrm{III}} = |\dot{\epsilon}|_{max}$) the shear strength, $(\sigma_{\mathrm{I}} - \sigma_{\mathrm{III}})_f/2$, depends on the value of k and may be found analytically by locating the stress point on the yield surface for which the associated plastic flow rate (i.e. $\lambda\{\partial f/\partial\sigma_1, \partial f/\partial\sigma_2, \partial f/\partial\sigma_3\}^T$) is perpendicular to one of the principal directions (i.e. $\partial f/\partial\sigma_i = 0$ where i is 1, 2 or 3). The relevant analytical expression for this condition is implicit and requires a numerical root search for solution. Fig. 4 shows the solution of this root search problem as a function of k. The figure shows the ratio of soil strength values, in terms of the radius of the largest Mohr circle, $(\sigma_{\mathrm{I}} - \sigma_{\mathrm{III}})_f/2$, to the undrained strength in triaxial compression, s_u. In addition to the plane strain condition, Fig. 4 shows the value of triaxial compression and extension. Note that for these modes of straining this is also the ratio of plastic work rate between the new model and Tresca model. As can be seen, the plane strain strength and dissipation are higher than those of Tresca, reaching the value of von Mises when $k = 1$ (with strength roughly 15% higher than that of Tresca). Nonetheless, the difference from Tresca is smaller than 5% for k smaller than 0.8. This indicates that 2D calculations with this model should provide similar results to classical analyses with Tresca, yet capable of providing the lower strength for the 3D tunnel heading problem. One should remember that the strain condition along discontinuities is that of plane strain, and therefore the utilization of the above asymmetric yield function does not offer any advantage to classical upper bound mechanisms involving deformation of multiple rigid bodies (deforming at their interfaces), as it will result in a similar dissipation rate to that of Tresca, yet it is of importance if one wishes to retrieve the 2D solution.

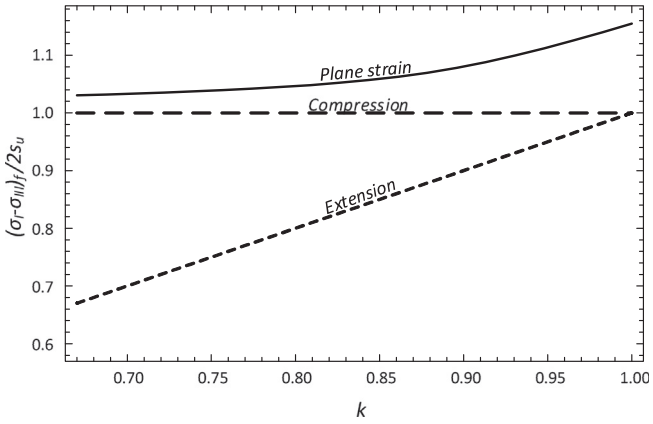

Fig. 4. Normalized soil strength values as function of k.

The fact that dissipation along discontinuities is that of plane strain (that is, excessive compared to extension) highlights the importance and advantage of incorporating continuous velocity fields, such as those of Klar et al. (2007) and Mollon et al. (2013), for upper calculations when using an asymmetric yield function.

3. Evaluation of upper bound values by BVP switch

The current work utilizes certain capabilities of the explicit time marching technique of FLAC^{3D} (Itasca, 2015) that can facilitate rigorous calculation of upper bound values. FLAC^{3D} has been previously used to establish stability numbers for tunnel face by bracketing the limit state through recursive analyses (e.g. Mollon et al., 2013). In the bracketing method, the limit state is identified by searching the highest load for which the system can still achieve a static equilibrium. In the explicit time marching scheme, a static equilibrium is defined when the accelerations, or the unbalanced forces, slowly diminish until they become negligible compared to the driving load. If the accelerations do not diminish, an unstable state is declared, and the load should be decreased (or the strength increased) to achieve the limit state. Through successive bracketing and intersections, the limit state can be calculated quite accurately. The bracketing method is well accepted in slope stability analysis, where the search is performed over the mobilized strength.

Although the bracketing approach can characterize the limit state quite efficiently, it does not constitute a rigorous upper bound solution, since it never involves a constant velocity field. That is, the velocity field either decelerates towards a static equilibrium or accelerates in the unstable state. Nonetheless, the mechanisms that naturally develop in the unstable state of the bracketing procedure can be used to generate kinematically admissible velocity fields for upper bound calculations by a few relatively simple steps. The unstable mechanisms in the bracketing method

Please cite this article in press as: Elkayam, I., & Klar, A., Upper bound of tunnel face stability using asymmetric yielding, Underground Space (2018), https://doi.org/10.1016/j.undsp.2018.03.001

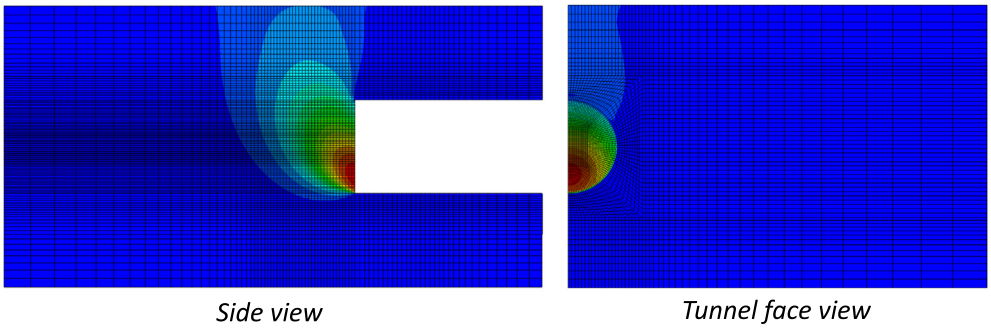

Fig. 5. Developed mechanism in case of $\beta = 4, C/D = 1$ and $P/D = 0$.

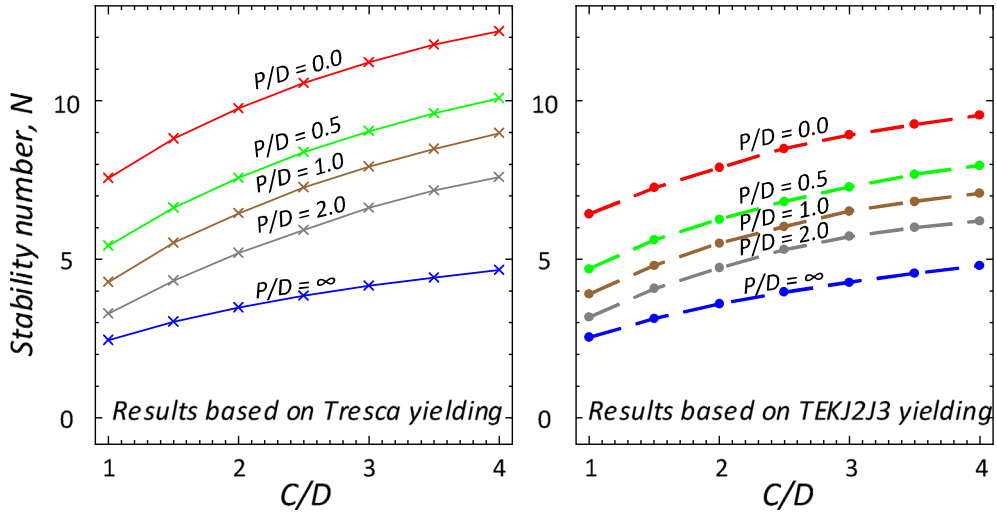

Fig. 6. Upper bound stability numbers as function of P/D and C/D (for $\beta = 0$): (a) results based on Tresca yield function, (b) results based on asymmetric (TEKJ2J3) yield function (with $k = 0.7$).

Table 1
Stability numbers based on Tresca dissipation and mechanism from the 'Tresca analysis'.

		C/D						
		1.0	1.5	2.0	2.5	3.0	3.5	4.0
P/D	0.0	7.56	8.81	9.76	10.56	11.21	11.77	12.19
	0.5	5.43	6.63	7.57	8.38	9.04	9.60	10.08
	1.0	4.28	5.52	6.45	7.27	7.92	8.48	8.98
	2.0	3.29	4.33	5.20	5.92	6.62	7.17	7.59
	∞	2.45	3.03	3.48	3.85	4.16	4.42	4.66

Table 2
Stability numbers based on TEKJ2J3 dissipation and mechanism from 'TEKJ2J3 analysis'.

		C/D						
		1.0	1.5	2.0	2.5	3.0	3.5	4.0
P/D	0.0	6.56	7.32	7.96	8.61	9.04	9.34	9.64
	0.5	4.75	5.64	6.30	6.87	7.32	7.78	8.09
	1.0	3.94	4.82	5.55	6.06	6.58	6.86	7.12
	2.0	3.22	4.11	4.79	5.33	5.77	6.06	6.24
	∞	2.52	3.12	3.58	3.96	4.28	4.55	4.80

Please cite this article in press as: Elkayam, I., & Klar, A., Upper bound of tunnel face stability using asymmetric yielding, Underground Space (2018), https://doi.org/10.1016/j.undsp.2018.03.001

Table 3
Stability numbers based on Tresca dissipation and mechanism from the 'TEKJ2J3 analysis'.

		C/D						
		1.0	1.5	2.0	2.5	3.0	3.5	4.0
P/D	0.0	8.32	9.46	10.42	11.29	11.92	12.40	12.86
	0.5	5.95	7.23	8.22	9.01	9.64	10.30	10.73
	1.0	4.73	6.09	7.07	7.92	8.62	9.10	9.48
	2.0	3.52	4.74	5.62	6.60	7.32	7.77	8.06
	∞	2.45	3.03	3.48	3.85	4.16	4.42	4.66

are associated with an accelerating velocity field (since the problem is load controlled in the search for limit state). An admissible collapse mechanism (with a constant velocity field) can be generated by converting the problem into a displacement or velocity controlled boundary value problem (BVP). This may be achieved by capturing the surface velocity profile in a given unstable state, and using it as a boundary condition for a new problem (involving elastic perfectly plastic soil behavior). The steady state (constant velocity) mechanism that develops in the new problem may constitute an admissible velocity field for a classical, and rigorous, upper bound calculation. In principle, if the procedure is performed on the verge of stability, the resulting upper bound solution may well represent the exact solution (in fact, one may consider the static case, on the verge of stability, as a lower bound).

For weightless soil, the solution can start with identifying the limit state surcharge using the bracketing method, and then switching the last unstable state into a velocity controlled BVP. Note that scaling down of the surface velocity field may be used to avoid numerical issues in the consecutive velocity controlled BVP.

For none zero weight soil, an initial stress condition should be defined to be in equilibrium with the gravitational forces. This includes stresses on the tunnel face, corresponding to the prescribed k_0 condition. The limit state surcharge can then be searched for, before switching to the velocity controlled BVP. In both cases, the velocity controlled BVP should be ran sufficiently long until a steady state velocity field develops. In the explicit scheme, this requires the use of a suitable damping scheme that removes stress waves, yet allows for the development of a constant velocity field. In fact, FLAC^{3D} incorporates, inherently, a damping scheme that acts only on reversal of velocity signs, such to allow the natural development of steady state plastic flow fields. Once the steady state develops there is either plastic flow or no flow, and the velocity field may be considered as rigid plastic.

Unlike simulations aiming to produce estimations of expected displacements and settlement troughs, the above approach is not sensitive to the location of the boundaries, provided that the developed collapse (plastic flow field) does not reach any of the boundaries. Providing smooth boundaries to the problem allows a convenient validation of this condition, such that if at the end of the calculation process the mechanism intersects the boundary the solution is invalid and the location of the boundary should be changed. As an example, Fig. 5 shows the mesh and the developed mechanism, using contours of normalized absolute velocity, in the case of $\beta = 4, C/D = 1$ and $P/D = 0$. As can be seen, the mechanism is found well within the limits of the model. The element size used in the current analyses ranged between $0.016D$ in the tunnel face to $0.3D$ away from the tunnel. Smaller elements could bring to a better (lower) upper bound solutions in case of shear bands development, representing discontinuities, but otherwise might not improve the solution by much.

The results provided in the following section are based on classical energy calculation, for which the dissipation of each point in space was calculated based on strain rates derived from the constant velocity field developed within FLAC^{3D} using the above approach. Appendix A provides the details of the energy calculation.

4. Results

Fig. 6 shows the upper bound values calculated using kinematically admissible velocity fields obtained from the above procedure for homogeneous soils. Fig. 6a shows results obtained from velocity fields generated by simulation incorporating the Tresca yield criterion, and energy calculations using the Tresca yield function as well. Fig. 6b shows the results obtained by a similar procedure only with the new asymmetric (TEKJ2J3) yield function using $k = 0.7$. Values presented in both figures may be considered strict upper bound values. As can be seen, for tunnel face stability (i.e. $P/D = 0$) the use of asymmetric yield function leads to significantly lower stability numbers than those of Tresca. As P/D increases the difference diminishes. This is because the mechanism becomes dominated by plane strain conditions as P/D increases. For $P/D = \infty$, and only for this case, the difference is exactly as that prescribed by the ratio presented in Fig. 4 between plane strain and compression shearing modes (3% for $k = 0.7$).

Tables 1 and 2 show the stability numbers of the Tresca and TEKJ2J3 collapse analyses, respectively. Since any zero volumetric strain mechanism is kinematically admissible for Tresca material, one can ask what is the upper bound value that is obtained when combining Tresca yielding (or dissipation) with the mechanism from the TEKJ2J3

Please cite this article in press as: Elkayam, I., & Klar, A., Upper bound of tunnel face stability using asymmetric yielding, Underground Space (2018), https://doi.org/10.1016/j.undsp.2018.03.001

solution. It would, however, be expected that the resultant upper bound value would be greater than that based on Tresca yielding together with the mechanism that was derived for Tresca material, considering the approach yields the exact value, or close to the exact value. If the results are minorly higher, than it may be concluded that the mechanisms are similar. Table 3 provide these values, and as can be seen, except for the plane strain case, the values are significantly greater than those provided in Table 1. This indicates that the TEKJ2J3 mechanism is different than the mechanism achieved from the Tresca model for the 3D collapse. For the 2D case, the mechanisms are essentially the same.

Fig. 7 shows a comparison between the TEKJ2J3 upper bound values (i.e. right of Fig. 6) and the commonly used design curves of Kimura and Mair (1981). As can be seen the new results agree well with the commonly used design values, while located significantly below the range for upper bound values based on Tresca material (seen in Fig. 1).

Further analyses were performed to include the effect of gravitation. Fig. 8 shows results for the extreme case of $P/D = 0$, for different values of normalized weight, expressed by $\beta = \gamma D/s_u$. For $\beta = 2$ the values of the stability numbers are slightly lower than those of $\beta = 0$. For $\beta = 4$ the values are also smaller for low C/D, but become greater than those of $\beta = 0$ with increasing C/D. Nonetheless, the difference throughout the complete range is smaller than 8%.

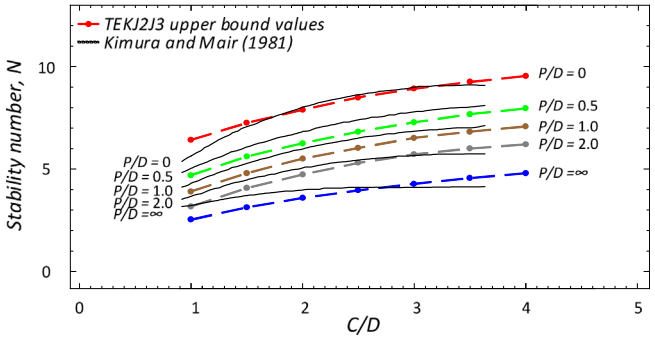

Fig. 7. Comparison between TEKJ2J3 upper bound values (using $k = 0.7$) and Kimura and Mair (1981) empirically based design curves.

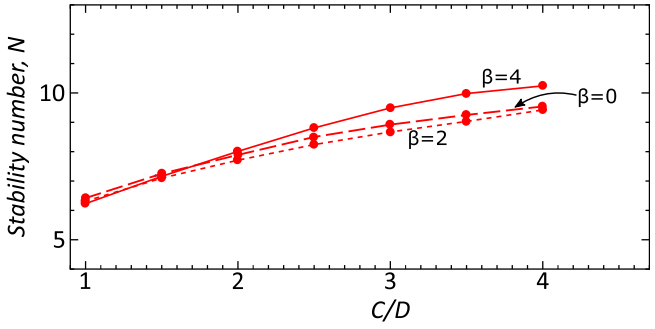

Fig. 8. Comparison between different β values for $P/D = 0$.

5. Summary and conclusions

Significant effort has been invested over recent years in attempts to produce more accurate upper bound mechanisms that will minimize the gap that exists between analytically and experimentally based stability numbers for tunnel face stability, yet the gap persists. This paper suggests that this may well be the outcome of the fact that upper bound calculations are commonly performed using Tresca yield criterion which provides equal dissipation (and strength) in all shearing modes (compression, extension and plane strain), while the mechanisms of tunnel face collapse are governed by an extension shearing mode, commonly associated with a lower strength. There may well be other reasons such as anisotropy, but certainly shearing mode is of importance. It should be noted that resolution of the matter through incorporation of the 'extension undrained shear strength' for the s_u value in Tresca yield criterion is inappropriate, and that the solution cannot be considered an upper bound (simply because it may underestimate strength, and dissipation, for soil elements which are not in pure symmetric extension). Consequently, this paper suggested the use of an asymmetric yield function for the evaluation of tunnel face stability in undrained clay. The yield function provides lower undrained shear strength, and dissipation, in extension mode of shearing, and similar undrained strength values in compression and plane strain shearing when compared to Tresca. Using a new technique, that switches between load controlled BVP to velocity controlled BVP, at the limit state of collapse, kinematically admissible fields were generated numerically, and used for conventional upper bound analyses, both with Tresca yield criterion and with TEKJ2J3. For tunnel face stability ($P/D = 0$) the obtained upper bound values are significantly smaller than those obtained with Tresca material while for plane strain mechanisms ($P/D = \infty$) are essentially similar. The new upper bound values agree well with the empirically based design curves of Kimura and Mair (1981) (commonly used for design).

Appendix A. Energy calculation

Let us consider two orthogonal axes within the π-plane shown in Fig. A.9, one vertical (appearing to coincide with σ_1) and one horizontal, denoted by F and E. The plastic strain corresponding to these axes are:

$$\dot{\epsilon}_E = \frac{\dot{\epsilon}_{max} + 2\dot{\epsilon}_{min}}{\sqrt{2}} \tag{A.1}$$

$$\dot{\epsilon}_F = \sqrt{\frac{3}{2}}\dot{\epsilon}_{max} \tag{A.2}$$

where $\dot{\epsilon}_{min}$ is the minimal principal strain rate, and $\dot{\epsilon}_{max}$ is the maximal principal strain rate. Note that the strain normal to the π-plane is zero. The yield function can be represented by stresses plotted in the π-plane, using σ_F and σ_E:

Please cite this article in press as: Elkayam, I., & Klar, A., Upper bound of tunnel face stability using asymmetric yielding, Underground Space (2018), https://doi.org/10.1016/j.undsp.2018.03.001

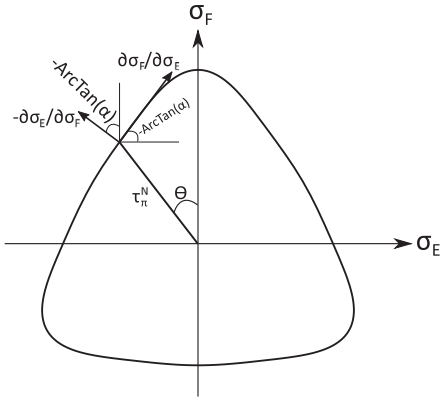

Fig. A.9. Geometrical relationship α and $\tan(\theta)$ in the π-plane.

$$\sigma_F = s_u \tau_\pi^N(\theta)\cos\theta \tag{A.3}$$

$$\sigma_E = -s_u \tau_\pi^N(\theta)\sin\theta \tag{A.4}$$

$$\tau_\pi^N(\theta) = \sqrt{\frac{8}{3}}\left(1 - \frac{3}{2}(1-k)\frac{1-\cos(3\theta)}{2-\cos(3\theta)}\right) \tag{A.5}$$

where θ is angle between the resultant stress in π plane and σ_F and τ_π^N is a normalized distance on the π-plane. Under associative plastic flow,

$$\frac{\dot{\epsilon}_E}{\dot{\epsilon}_F} = \alpha = -\frac{\partial\sigma_F}{\partial\sigma_E} = -\frac{\partial\sigma_F/\partial\theta\cdot d\theta}{\partial\sigma_E/\partial\theta\cdot d\theta} = -\frac{\partial\sigma_F/\partial\theta}{\partial\sigma_E/\partial\theta} \tag{A.6}$$

where α is a ratio between the strain rate ratios. α is equal to the tangent of the plastic flow direction. For a given k value, α is only a function of θ. Fig. A.10 shows the relation between α and $\tan(\theta)$ for various k values. Clearly for $k = 1$ an identity exists between α and -tan(θ) as the yield function becomes that of von Mises. It is convenient to present the relation as $\theta = f_\theta(\alpha)$, for energy calculations.

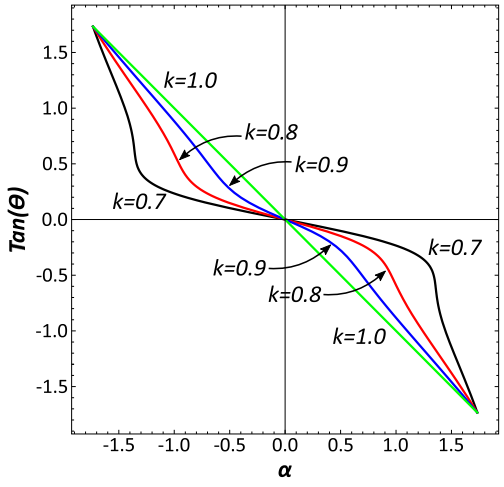

Fig. A.10. Relationship between α and $\tan(\theta)$.

The density of internal dissipation is therefore:

$$\dot{I} = \sqrt{\frac{3}{2}}\dot{\epsilon}_{max} s_u \tau_\pi^N(f_\theta(\alpha))[\cos(f_\theta(\alpha)) - \alpha\sin(f_\theta(\alpha))]$$
$$\alpha = \frac{\dot{\epsilon}_{max} + 2\dot{\epsilon}_{min}}{\sqrt{3}\dot{\epsilon}_{max}} \tag{A.7}$$

If an upper bound value is evaluated for $\sigma_S - \sigma_T$ then the stability value from the energy calculation is:

$$N = \frac{\int_V \dot{I}dV - \frac{\beta}{D}\int_V v_v dV}{\int_s v_v dS} + \beta\frac{C + D/2}{D} \tag{A.8}$$

where v_v is the vertical velocity, and s is the surface. The above surface and volumetric integral were calculated numerically, using the domain subdivision of FLAC^{3D} into constant strain tetrahedral elements. Results based on the direct energy calculations using only strain rates from the velocity field were in excellent agreement with energy calculations using the internal plastic strains and stresses (derived from the elastic-perfectly plastic law written for FLAC^{3D}), with a difference smaller than 2%.

References

Atkinson, J., & Potts, D. (1977). Stability of a shallow circular tunnel in cohesionless soil. *Geotechnique, 27*(2), 203–215.

Augarde, C. E., Lyamin, A. V., & Sloan, S. W. (2003). Stability of an undrained plane strain heading revisited. *Computers and Geotechnics, 30*(5), 419–430.

Campanella, R. G., & Vaid, Y.P. (1973). Influence of stress path on the plane strain behaviour of sensitive clay. In *Proceedings of the 8th international conference on soil mechanics and foundation engineering. Moscow* (pp. 85–92).

Davis, R. O., & Selvadurai, A. P. S. (2005). *Plasticity and geomechanics.* Cambridge, UK: Cambridge University Press.

Davis, E. H., Gunn, M. J., Mair, R. J., & Seneviratine, H. N. (1980). The stability of shallow tunnels and underground openings in cohesive material. *Géotechnique, 30*(4), 397–416.

Duncan, J. M., & Seed, H. B. (1966). Strength variations along failure surfaces in clay. *Journal of the Soil Mechanics and Foundations Division, 92*(6), 81–104.

Gasparre, A. (2005). *Advanced laboratory characterisation of London clay* (Ph.D. thesis). Imperial College London.

Itasca. (2015). Fast Lagrangian Analysis of Continua in 3 Dimensions Ver. 5. User manual.

Kimura, T., & Mair, R. J. (1981). Centrifugal testing of model tunnels in soft clay. In *Proceedings of the 10th international conference on soil mechanics and foundation engineering. Stockholm* (Vol. 1, pp. 319–322).

Klar, A., & Elkayam, I. (2017). Tunnel face stability curves considering asymmetric yielding. In *EURO:TUN 2017, 4th international conference on computational methods in tunnelling and subsurface engineering, 18–20 Apr 2017, Innsbruck, Austria* (pp. 75–82).

Klar, A., & Klein, B. (2014). Energy-based volume loss prediction for tunnel face advancement in clays. *Géotechnique, 64*(10), 776–786.

Klar, A., & Osman, A. S. (2008). Load-displacement solutions for piles and shallow foundations based on deformation fields and energy conservation. *Géotechnique, 58*(7), 581–589.

Klar, A., & Randolph, M. F. (2008). Upper-bound and load displacement solutions for laterally loaded piles in clays based on energy minimisation. *Géotechnique, 58*(10), 815–820.

Klar, A., Osman, A. S., & Bolton, M. D. (2007). 2D and 3D upper bound solutions for tunnel excavation using 'elastic' flow fields. *International Journal for Numerical and Analytical Methods in Geomechanics, 31*(12), 1367–1374.

Leca, E., & Dormieux, L. (1990). Upper and lower bound solutions for the face stability of shallow circular tunnels in frictional material. *Géotechnique, 40*(4), 581–606.

Please cite this article in press as: Elkayam, I., & Klar, A., Upper bound of tunnel face stability using asymmetric yielding, Underground Space (2018), https://doi.org/10.1016/j.undsp.2018.03.001

Mair, R. J. (1979). *Centrifugal modelling of tunnel construction in soft clay* (Ph.D. thesis). Cambridge University.

Mollon, G., Dias, D., & Soubra, A. (2010). Face stability analysis of circular tunnels driven by a pressurized shield. *Journal of Geotechnical and Geoenvironmental Engineering, 136*(1), 215–229.

Mollon, G., Dias, D., & Soubra, A. (2013). Continuous velocity fields for collapse and blowout of a pressurized tunnel face in purely cohesive soil. *International Journal for Numerical and Analytical Methods in Geomechanics, 37*(13), 2061–2083.

Nishimura, S. (2005). *Laboratory study on anisotropy of natural London clay* (Phd thesis). Imperial College London.

Osman, A. S., Mair, R. J., & Bolton, M. D. (2006). On the kinematics of 2D tunnel collapse in undrained clay. *Géotechnique, 56*(9), 585–595.

Pan, Q., & Dias, D. (2016). Face stability analysis for a shield-driven tunnel in anisotropic and nonhomogeneous soils by the kinematical approach. *International Journal of Geomechanics ASCE, 16*(3), 1–11. https://doi.org/10.1061/(ASCE)GM.1943-5622.0000569.

Sloan, S. W., Assadi, A. (1993). Stability of shallow tunnels in soft ground. In *Predictive soil mechanics: Proceedings of the wroth memorial symposium held at St. Catherine's College, Oxford, 27–29 July 1992* (pp. 644–663).

Wilson, D. W., Abbo, A. J., Sloan, S. W., & Lyamin, A. V. (2013). Undrained stability of a square tunnel where the shear strength increases linearly with depth. *Computers and Geotechnics, 49*, 314–325. https://doi.org/10.1016/j.compgeo.2012.09.005.

Xiang, Y., & Song, W. (2017). Upper-bound limit analysis of shield tunnel stability in undrained clays using complex variable solutions for different ground-loss scenarios. *International Journal of Geomechanics, 17*(9), 04017057. https://doi.org/10.1061/(ASCE)GM.1943-5622.0000946.

Zhang, C., Han, K., & Zhang, D. (2015). Face stability analysis of shallow circular tunnels in cohesive frictional soils. *Tunnelling and Underground Space Technology, 50*, 345–357. https://doi.org/10.1016/j.tust.2015.08.007.

Zhang, F., Gao, Y. F., Wu, Y. X., & Zhang, N. (2017). Upper-bound solutions for face stability of circular tunnels in undrained clays. *Géotechnique*, 1–10. https://doi.org/10.1680/jgeot.16.T.028.

Please cite this article in press as: Elkayam, I., & Klar, A., Upper bound of tunnel face stability using asymmetric yielding, Underground Space (2018), https://doi.org/10.1016/j.undsp.2018.03.001